Energy Balance Model for Imagery and Electromagnetic Propagation

HENRY RACHELE AND ARNOLD TUNICK

U.S. Army Research Laboratory, Battlefield Environment Directorate, White Sands Missile Range, New Mexico

(Manuscript received 7 September 1993, in final form 22 November 1993)

ABSTRACT

The character of temperature and moisture gradients in the atmospheric surface layer is shown to be related to the intensity of visual distortions or "blurring" of images routinely detected by electo-optical systems and sensors. The authors are able to make quantitative approximations of the optical turbulence effect as represented by the refractive-index structure parameter C_n^2. Through the application of Monin–Obukhov similarity, the magnitudes of potential temperature and specific humidity gradients are determined using values of sensible and latent heat fluxes estimated from a semiempirical radiation and energy balance model. The model is constrained to require a minimum number of conventional meteorological inputs at a specific reference level (i.e., 2 m). These measurements include temperature, pressure, relative humidity, and wind speed. The model also requires a judgment of soil type and moisture (dry, moist, or saturated), cloud characteristics (tenths of cloud cover, opacity, and an estimate of cloud height), day of the year, time of day, and longitude and latitude of the site of interest. Model concepts and equations are presented and several sample results are illustrated. Model estimates of net radiation; sensible, ground, and latent heat fluxes; and C_n^2 are compared with measured values or values derived from measurements.

1. Introduction

The refractive-index structure parameter C_n^2 routinely appears in formulations used to characterize the effects of optical turbulence on imagery and electromagnetic (EM) propagation. For many optical systems this structure parameter corresponds with degradation of performance (Tatarski 1961; Fried 1967). Basic formulations of C_n^2 (Panofsky 1968; Tatarski 1961; Hill 1989; Andreas 1988; Wyngaard 1973; Wesely 1976) include the gradient of the real index of refraction as a coefficient, which in turn is a direct function of the gradients of temperature and moisture [preferably potential temperature and specific humidity, according to Tatarski (1961)]. Temperature and moisture gradients can be approximated from sensible and latent heat flux estimates, and these fluxes can be obtained from energy balance formulations.

Numerous radiation and energy balance models appear in the literature (Angus-Leppan and Brunner 1980; Webb 1984; Campbell 1985; Pielke 1984; Danard et al. 1984; Yamada 1981; Carson 1987, to name a few), varying from comparatively simple to academically complex and requiring different amounts and numbers of inputs and computer capabilities. In this article we present a semiempirical model that was developed for specific battlefield applications, constrained by an operational limitation that a minimum of atmospheric information is available. Once the model was developed, we recognized that it may have other applications, such as use in agriculture, transport and diffusion, and mesoscale modeling.

The primary outputs of the model are estimates of sensible and latent heat fluxes, which in turn are used for estimating gradients of potential temperature and specific humidity, making use of Monin–Obukhov (1954) similarity relations as advocated by Dyer (1974). These gradients are then used to approximate quantitative estimates of the refractive index structure parameter.

The remainder of this article comprises the following sections: model concept, model equations and procedure, sample results, discussion, and summary and conclusions.

2. Model concept

The model concept emerges from the following operational scenario. One is interested in engineering approximations of the intensity of optical turbulence as characterized by the structure parameter C_n^2 at an arbitrary site where minimal conventional atmospheric information is available for different times of one day. The day of interest is known, and the longitude and latitude of the site are known. The U.S. Department of Agriculture (USDA) soil maps may help to determine the soil type, and from the meteorological reports one has an estimate of soil wetness—that is, dry, moist,

Corresponding author address: Arnold Tunick, U.S. Army Research Laboratory, Battlefield Environment Directorate, Attn: AMSRL-BE-S, White Sands Missile Range, NM 88002-5501.
E-mail: atunick@wsmr-relay.arl.army.mil

or wet. If the soils taxonomy and meteorological reports are not available, however, one makes on-the-spot judgments by examining samples of soil from the surface to 10 cm below the surface. In addition to the soil judgment, one also makes a judgment of sky conditions—in particular, the amount of cloud cover, an estimation of cloud height, and the opacity of the cloud cover. From the above information one proceeds to estimate the net radiative flux, which is then partitioned into the sensible, ground, and latent heat fluxes using the convention and formulations of radiation and energy balance proposed by Carson (1987).

a. Radiation balance

Carson (1987) states that the net radiation flux R_N at the soil surface is equal to the sum of the net shortwave radiative flux R_{SN} and the net longwave radiative flux R_{LN}; that is,

$$R_N = R_{SN} + R_{LN}. \quad (1)$$

He defines $R_{S\downarrow}$ as the downward shortwave radiative flux, including both the direct solar flux and diffuse radiation from the sky. Some of the shortwave radiation is reflected at the earth's surface so that

$$R_{SN} = R_{S\downarrow} - \alpha R_{S\downarrow}, \quad (2)$$

where α is the surface shortwave reflectivity, commonly called albedo. Estimates of albedo, however, can be a complex function of soil type and color, vegetative cover, and the elevation angle of the sun. Values of α as a function of soil and vegetation are given in Table 1, mainly from an extensive compilation by Hansen (1993a) and Pielke (1984). The functional form of α relative to the sun's position that we employ in our model is given in section 3.

Carson (1987) also notes that if $R_{L\downarrow}$ is the downward longwave radiation and a' is the surface absorptivity to longwave radiation, then the net incoming flux from the atmosphere is $(a'R_{L\downarrow})$. Additionally, using Stefan's law, one can write the upward flux due to thermal emission at the earth's surface as $\epsilon\sigma T_g^4$, where T_g is the effective surface temperature, ϵ is the longwave emissivity at the surface, and σ is the Stefan–Boltzmann constant ($\sigma = 5.6697 \times 10^{-8}$ W m^{-2} K^{-4}). Hence, the net longwave radiative flux R_{LN} is

$$R_{LN} = a'R_{L\downarrow} - \epsilon\sigma T_g^4. \quad (3)$$

It is common practice to combine the definition of ϵ with Kirchhoff's law so that $a' = \epsilon$. However, ϵ varies with soil type, vegetation, and snow or water cover, as given in Table 2 from Pielke (1984).

TABLE 1. Typical values of albedo α for various surfaces.

Surface	α	Surface	α
Snow and ice		Urban (people influenced)	
Snow, fresh fallen	75–95	Road, blacktop	14
Snow, thawing	30–65	Road, stone	15
Snow, old	40–70	Road, dirt, wet	18
Snow, icy	75	Road, dirt, dry	35
Ice, gray	60	Road, clay, wet	20
Ice, white	75	Road, clay, dry	30
Ice, water covered	26	Road, asphalt, wet	10
Ice, light snow cover	31	Road, asphalt, dry	15
Ice, porous and melting	41	Parking lot, black top	8
Desert shrublands, snow covered	18–19	Concrete, new, white	37
Conifer forest, snow covered	59–67	Buildings	9
Mixed forest, 50-cm snow cover	20	Developed urban area (average)	15
Grasslands, snow covered	46–50	Roof, thatched, new	20
Crops, snow covered	18–19	Roof, thatched, old	15
Tundra, snow covered	59–67	Roof, tiled, dirty	8
Soils and rocks		Crops, natural terrain, and vegetation	
Soil, dark, plowed, wet	6	Fallow field, wet	5–7
Soil, dark, plowed, dry	8	Fallow field, dry	8–12
Soil, light, plowed, wet	8	Spring wheat	10–25
Soil, light, plowed, dry	16	Winter wheat	16–23
Soil, dark, wet	8	Rice paddy	12
Soil, dark, dry	13	Sugar cane	15
Soil, light, wet	10	Cocoa	16
Soil, light, dry	18	Ground nuts	17
Dark organic soils	10	Winter rye	18–23
Dark gray silt	12	Beets	18
Red soils	17	Maize	18
Brown soils	17	Tobacco	19
Clay, wet	16	Potatoes, yams	19
Clay, dry	23	Alfalfa	23–32
Loam, wet	16	Cotton	20–22
Loam, dry	23	Sorghum	20
Clay loam, wet	19	Lettuce	22
Clay loam, dry	13	Forest, coniferous	5–15
Sandy soil, wet	20	Forest, deciduous	10–20
Sandy soil, dry	25	Grass, green	26
Sand, white, wet	25	Meadows, green	10–20
Sand, white, dry	35	Coniferous trees, dormant	12
Peat soils	5–15	Deciduous trees, dormant	12
Lime	45	Tall grass, dormant	13
Gypsum	55	Mowed grass, dormant	19
Lava	10	Tundra	15–20
Granite	12–18	Savanna	15
Rock, wet	20	Steppe	20
Rock, dry	35	Sand dune, wet	20–30
Stone	30	Sand dune, dry	35–45

From Hansen (1993a) and Pielke (1984).

b. Surface energy balance

Carson (1987) writes the energy flux balance at the soil surface as

$$R_N = H + L'E + G, \quad (4)$$

where R_N is the net radiative flux, H is the turbulent sensible heat flux, $L'E$ is the latent heat flux due to surface evaporation, and G is the flux of heat into the soil. Equations for R_N, H, and G are given in section

TABLE 2. Typical values of emissivity ϵ for various surfaces.

Ground cover	ϵ
Fresh snow	0.99
Old snow	0.82
Dry sand	0.95
Wet sand	0.98
Dry peat	0.97
Wet peat	0.98
Soils	0.9–0.98
Asphalt	0.95
Concrete	0.71–0.9
Tar and gravel	0.92
Limestone gravel	0.92
Light sandstone rock	0.98
Desert	0.84–0.91
Grass lawn	0.97
Grass	0.90–0.95
Deciduous forests	0.95
Coniferous forests	0.97
Urban area (range)	0.85–0.95

From Pielke (1984).

3. Latent heat flux estimates are calculated as a residual using Eq. (4). We chose positive values of R_N and G to represent fluxes directed downward, while positive H and $L'E$ values represent fluxes directed away from the air–soil interface.

3. Equations and procedures

a. Shortwave solar radiation

The formulations we use to compute the incoming shortwave solar radiation for cloudless skies are patterned after Meyers and Dale (1983). These are then augmented with empirical results by Haurwitz (1945) to account for cloudy skies.

For clear skies Meyers and Dale (1983) write

$$R_{S\downarrow} = I = I_0 T_R T_g T_w T_a \cos Z, \tag{5}$$

where I_0 is the extraterrestrial flux density at the top of the atmosphere on a surface normal to the incident radiation, Z is the solar zenith angle, and T_i are the transmission coefficients for Rayleigh scattering (R), absorption by permanent gases (g), water vapor (w), and absorption and scattering of aerosols (a).

The incident radiation I_0 (W m^{-2}) changes throughout the year because of changes in the earth–sun distance and is adjusted by using the equation

$$I_0 = 1353\left\{1 + 0.034 \cos\left[\frac{2\pi(n' - 1)}{365}\right]\right\}, \tag{6}$$

where n' is the Julian day. The solar zenith angle is computed by using

$$Z = \cos^{-1}[\sin(\delta)\sin(D) + \cos(\delta)\cos(D)\cos(H')], \tag{7}$$

where δ is the latitude, D the declination angle, and H' is the solar hour angle. The solar declination angle, computed using formulations by Woolf (1968), is expressed as

$$\sin D = \sin(23.4438)\sin\beta, \tag{8}$$

where β (°) is

$$\beta = \gamma + 0.4087\sin(\gamma) + 1.8724\cos(\gamma) - 0.0182\sin(2\gamma) + 0.0083\cos(2\gamma), \tag{9}$$

and γ (°) is

$$\gamma = 279.9348 + d. \tag{10}$$

The angle d is the angular fraction of a year represented by a particular date. The angle d may be calculated by

$$d = (\text{number of day of year} - 1)\left(\frac{360}{365.242}\right). \tag{11}$$

The solar hour angle H' (°) is a measure of the longitudinal distance from the sun to the point of calculations given by

$$H' = 15(T - M) - \eta, \tag{12}$$

where T is time (UTC) of the calculations, M is the time in hours after midnight of the passage of the sun over the Greenwich meridian or true solar noon, and η is longitude, counted positive west of Greenwich. In terms of d defined in Eq. (11), M is

$$M = 12.0 + 0.12357\sin(d) - 0.004289\cos(d) + 0.153809\sin(2d) + 0.060783\cos(2d). \tag{13}$$

The solar hour angle H' that relates to sunrise and sunset is found using Eq. (7) as

$$H' = \cos^{-1}\left(\frac{\sin A - \sin\delta\sin D}{\cos\delta\cos D}\right), \tag{14}$$

where A is the sunrise–sunset solar elevation angle. At ground level Woolf sets $A = -0.9°$. The solar day extends from $M - H'$ to $M + H'$, and hence sunrise time is $M - H'$, and sunset time is $M + H'$.

An empirical equation for $T_R T_g$ in Eq. (5) by Kondratyev (1969) and modified by Atwater and Brown (1974) to include forward scattering is

$$T_R T_g = 1.021 - 0.084 \times [m(949P \times 10^{-5} + 0.051)]^{1/2}, \tag{15}$$

where P is the surface pressure (kPa), and m is the optical air mass at a pressure of 101.3 kPa given by

$$m = 35[1224\cos^2(Z) + 1]^{-1/2}, \tag{16}$$

where Z is the zenith angle. An expression for computing the broadband transmission of water vapor absorption by McDonald (1960) is

$$T_w = 1 - 0.077(um)^{0.3}, \tag{17}$$

TABLE 3. Seasonal and latitudinal mean values of λ.

Latitudinal zone (°N)	Season				Annual average
	Winter	Spring	Summer	Fall	
0°–10°	3.37	2.85	2.80	2.64	2.91
10°–20°	2.99	3.02	2.70	2.93	2.91
20°–30°	3.60	3.00	2.98	2.93	3.12
30°–40°	3.04	3.11	2.92	2.94	3.00
40°–50°	2.70	2.95	2.77	2.71	2.78
50°–60°	2.52	3.07	2.67	2.93	2.79
60°–70°	1.76	2.69	2.61	2.61	2.41
70°–80°	1.60	1.67	2.24	2.63	2.03
80°–90°	1.11	1.44	1.94	2.02	1.62
Northern Hemisphere average	2.52	2.64	2.62	2.70	2.61

From Smith (1966).

where m is the optical air mass (defined above), and u, the precipitable water vapor, is determined by using an expression by Smith (1966); that is,

$$u = \frac{PW_r}{g(\lambda + 1)}, \quad (18)$$

where P is the pressure near the earth's surface (i.e., 2 m), W_r is the near-surface mixing ratio, g is the acceleration due to gravity, and λ (see Smith 1966) is given in Table 3.

A simple treatment used by Meyers and Dale (1983) for estimating T_a was proposed by Houghton (1954) and is expressed as

$$T_a = X^m, \quad (19)$$

where m is the optical mass, and X is an empirically derived constant (on the order of 0.935).

Finally, to account for the effect of clouds, we introduce a transmission coefficient derived empirically by Haurwitz (1945). Haurwitz computed the ratio of insolation with partly or completely covered sky to insolation of cloudless skies, as shown in Table 4. We use Table 4 to correct our estimates of insolation for cloud cover since Eq. (16) gives the air mass as a function of solar zenith angle, and from local observations one can determine cloud amount and opacity.

At this point we have formulations for computing the incoming shortwave solar radiation $R_{S\downarrow}$, which is then adjusted for albedo. As indicated in Table 1, albedo is a function of soil type and color, moisture, vegetation, and solar elevation angle. Although the first four effects are reflected in Table 1, the last is computed by using an approximation by Paltridge and Platt (1976); that is,

$$\alpha(Z) = \alpha_1 + (1 - \alpha_1)\exp[-k'(90° - Z)], \quad (20)$$

where k' is of order 0.1, Z is the solar zenith angle, and α_1 is the small zenith angle value of albedo (i.e., generally the values of albedo found in Table 1).

b. *Downward longwave radiation*

Gates (1965) offers an expression for downward longwave radiation for clear skies based on an empirical relationship by Swinbank (1963), which is expressed as

$$R_{L\downarrow} = -170.9 + 1.195\sigma T_r^4, \quad (21)$$

where $R_{L\downarrow}$ is in watts per square meter, $\sigma = 5.6697 \times 10^{-8}$ W m^{-2} K^{-4}, and T_r is the reference-level (i.e., 2 m) temperature in kelvins. Paltridge and Platt (1976), in turn, suggest an addition to Eq. (21) to account for clouds, giving a total expression of

$$R_{L\downarrow} = -170.9 + 1.195\sigma T_r^4 + 0.3\epsilon_c\sigma T_c^4(\text{cc}), \quad (22)$$

where ϵ_c, the longwave flux emissivity given in Table 5, is the emissivity of the cloud base, T_c is the temperature of the cloud base in kelvins, and cc is the cloud amount in tenths. With an estimate of the cloud height, one can approximate T_c, assuming an average of the dry- and moist-adiabatic lapse rate. From recent experience, we have found that the empirically based constant in Eqs. (21) and (22) can be adjusted to obtain improved radiation estimates before sunrise and after

TABLE 4. Ratio (%) of insolation with partly or completely cloud-covered sky to the insolation with cloudless sky.

Cloud amount (tenths)	1–3				4–7			8–9			10				
Opacity	0	1	2	3	1	2	3	1	2	3	0	1	2	3	4
Air mass															
1.0	104	103	98	88	98	93	88	92	76	68	87	80	60	31	18
1.5	99	100	97	90	96	89	83	92	75	65	88	79	58	30	19
2.0	94	98	96	92	94	85	78	92	75	63	88	79	55	28	20
2.5	90	96	94	94	92	81	74	92	74	60	89	79	52	27	20
3.0	85	94	92	96	90	78	69	93	74	58	89	79	50	27	21
3.5	81	92	90	98	87	74	65	93	73	56	90	79	47	25	21
4.0	77	90	89	100	84	71	61	93	72	54	90	79	46	25	22
4.5	73	88	87	102	82	67	58	93	72	52	91	79	44	24	23
5.0	70	86	85	104	80	64	54	93	72	50	91	79	41	23	23

From Haurwitz (1945).

TABLE 5. Longwave flux emissivity ϵ_c.

Cloud level	Cloud type	ϵ_c
1	Cirrus	0.3
2	Altocumulus–altostratus	0.9
3	Low cloud 2	1.0

From Paltridge and Platt (1976).

sunset. We have had some success modifying its value from −170.9 to −130.0.

c. Upward longwave radiation

The upward longwave radiative flux $R_{L\uparrow}$ is computed by using a formulation from Yamada (1981) and is expressed as

$$R_{L\uparrow} = \epsilon\sigma T_g^4 + (1 - \epsilon)R_{L\downarrow}, \tag{23}$$

where ϵ is the surface emissivity (see Table 2), and σ is the Stefan–Boltzmann constant. To evaluate Eq. (23) one requires an estimate of the effective ground temperature T_g. This is achieved through the application of Monin–Obukhov (1954) similarity and the flux-gradient hypothesis as advocated by Dyer (1974).

For unstable surface-layer conditions, we assume that a semiempirical expression of the sensible heat flux H given by Angus-Leppan (1971) [based on the Penman (1948) combination form] is adequate as a first approximation for clear sky, dry ground conditions; that is,

$$H = 450 \sin\phi_e, \tag{24}$$

where ϕ_e is the solar elevation angle ($\phi_e = 90 - Z$).

For stable conditions, we assume that H is constant and negative in sign (and generally an order of magnitude less than its daytime peak value). Although this assumption is relatively weak in attempting to model the complexities of the sensible heat flux and its associated surface-layer temperature gradient structure during stable conditions, it does allow us to apply our modeling techniques to a 24-h dataset with a greater degree of practicality. Commonly, however, the sensible heat flux will remain relatively flat or uniform in the stable surface layer (Angus-Leppan 1971).

Having a first estimate for H, we compute the similarity forms for the Obukhov length L and friction velocity u_* using

$$L = \frac{-u_*^3 c_p \rho \theta_{vr}}{kgH}, \tag{25a}$$

where c_p is the specific heat of air (c_p = 1004.6 J K^{-1} kg^{-1}), ρ is the density of air, θ_{vr} is the reference-level virtual potential temperature ($\theta_{vr} = \theta_r + 0.61q_r$, where θ_r and q_r are the reference-level potential temperature and specific humidity, respectively), k is von Kármán's constant (0.4), and g is acceleration due to gravity. Given moisture input as relative humidity RH, we alternatively determine q_r as described by Rogers (1979); that is,

$$q_r = 3.8 \times 10^{-3} \frac{\text{RH}}{100} \times \exp\left[5.44 \times 10^3 \left(\frac{1}{273.15} - \frac{1}{T_r}\right)\right]. \tag{25b}$$

We introduce our expression for u_*, the friction velocity, which we have shown to be equivalent to that of Paulson (1970) and Benoit (1977), and which we express as

$$u_* = \frac{V_r k}{\{\ln[(x-1)/(x+1)] + 2\tan^{-1}x\}_{z_0}^{z-d}}, \tag{26a}$$

where V_r is the reference-level wind speed, $x = [1 - 15(z/L)]^{1/4}$ for unstable conditions, and $x = 1 + 5(z/L)$ for stable conditions. For neutral conditions,

$$u_* = V_r k \left(\ln\frac{z-d}{z_0}\right)^{-1}. \tag{26b}$$

In Eqs. (26a) and (26b), z_0 is the roughness length for momentum, and d is the displacement height. We approximate values for these parameters as $z_0 = 0.14z_e$ and $d = 0.7z_e$, where z_e is referred to as the height of the roughness element or the average height of the terrain or ground cover (surface vegetation) present. Table 6 represents an extensive compilation by Hansen (1993b) of typical roughness length values for various surfaces. Solving Eqs. (25a), (25b), and (26a) or (26b) iteratively, we obtain values for L and u^* for the approximated value of H.

Also, from similarity forms we can write

$$\theta_* = \frac{u_*^2 \theta_{vr}}{kgL}. \tag{27}$$

Hence, we can compute a first estimate for θ_*, the potential temperature scaling constant, which can be used to approximate T_g, the apparent surface temperature, since

$$T_g = T_r - \frac{\theta_*}{k}\left[\ln\left(\frac{y-1}{y+1}\right)\right]_{z_h}^{z-d}, \tag{28a}$$

where near the earth's surface $T_r \approx \theta_r$, $y = [1 - 15(z/L)]^{1/2}$ for unstable conditions, and $y = 1 + 5(z/L)$ for stable conditions. For neutral conditions,

$$T_g = T_r - \frac{\theta_*}{k}\left(\ln\frac{z-d}{z_h}\right). \tag{28b}$$

To evaluate Eqs. (28a) or (28b), however, we require an estimate of z_h, the roughness length for temperature. Although a somewhat more desirable expression is given by Verma (1989), in practice we commonly approximate $z_h = 0.13z_0$ at all times of the day including

transition or neutral periods. With an estimate of T_g for dry cloudless conditions, we compute $R_{L\uparrow}$. From the above equations (sections 3a, 3b, and 3c), we can compute the first estimate of net radiation; that is, $R_N = R_{SN} + R_{LN}$.

d. Ground heat flux

We express the ground heat flux as

$$G = -G^* + (T_g - T_{gn})K_0 \sin\left[\frac{\pi}{12}(t - t_n)\right], \quad (29a)$$

where

$$G^* = (T_{g(t_n+2)} - T_{gn})K_0 \sin\left(\frac{2\pi}{12}\right). \quad (29b)$$

Here T_{gn} is the ground temperature during adiabatic conditions (approximately 1 h after sunrise), t_n is the time (relative to midnight) of adiabatic conditions, $K_0 = K_s/2K^{1/2}$ for soil type and wetness, K_s is the soil thermal conductivity (W m^{-1} K^{-1}), and K is the soil thermal diffussivity (m^2 h^{-1}). Equations (29a) and (29b) are our modifications to the expressions for ground heat flux given by Angus-Leppan and Brunner (1980). Table 7 contains values of the thermal constants K_s and K.

Equation (29b) implies that the ground heat flux is zero approximately 2 h after the neutral (adiabatic) period. More recent experience confirms that the morning transition period may be approximated by $T_{\text{sunrise}} + 1$ h, and that G^* can often be set to a constant value (i.e., $G^* \approx 12.0$–15.0).

At this point we have all the equations necessary for computing a second approximation for H, assuming that for clear skies and dry ground conditions the latent heat flux is negligible; that is, $H = R_N - G$. The key to our computational procedure is that we complete an iterative process to determine what we refer to as a "dry and clear sky" sensible heat flux H_d. Our computations then proceed wherein we consider cloud-cover effects on the net radiative flux, effects of varying soil moisture on ground heat storage, and cloud-cover, evaporation, and wind speed effects on sensible heat flux estimates. Given H_d (the dry and clear sky value), we return to the expression given by Angus-Leppan (1971); that is,

$$H = CWH_d, \quad (30)$$

where C and W are correction factors to account for cloud cover and ground wetness. These reduction fractions are given in Fig. 1. In other words, we will scale our approximated H_d (dry and clear sky) using the appropriate values for C and W. We are then able to recompute the sensible heat flux, the surface temperature T_g, the net radiation, and the ground heat flux (remembering to change the constants given in Table 7 to reflect the level of soil wetness) to reflect local conditions (i.e., sky cover and soil moisture). Finally, the latent heat flux $L'E$ is determined as

TABLE 6. Typical values of roughness length z_0 for various surfaces.

Type of surface	z_0 (cm)
Ice	0.001
Smooth mudflats	0.001
Dry lake bed	0.003
Tundra, snow covered	0.01
Tundra, patchy snow	0.03
Tundra, after snowmelt	0.40
Tundra, midsummer	2.40
Snow cover (i.e., Antarctic)	0.01
Calm open sea	0.01
Desert, smooth	0.03
Grass, closely mowed	0.10
Grass, short	0.14
Farmland, snow covered	0.20
Bare soil, tilled	0.20–0.60
Nebraska prairie	0.70
Sparse grass, 10 cm high	0.70
Thick grass, 5–6 cm high	0.75
Grassy plains, level topography	1.0
Kansas prairie	1.0
Low shrubs, level topography	2.6
Grasslands, 18 cm high	2.7
Uncut grass w/isolated trees	3.0
Grass and trees, mixed	3.5
Sparse brush, semiarid	5.0
Sparse grass, 50 cm high	5.0
Thick grass, 50 cm high	9.0
Thick grass, 60–70 cm high	8.0–15.0
Brush, scrub growth, open	16.0
Brush, scrub growth, dense	25.0
Wooded country, level topography	40.0
Forested plateau, level topography	70.0–120.0
Forested plateau, rolling hills	120.0–130.0
Low mountains, hills, unforested	75.0
Subtropical savanna, grass, few trees	31.0–41.0
Subtropical savanna, grass w/many shrubs	51.0–61.0
Coniferous forest	110.0
Alfalfa	2.7
Cashew orchard, 2 m high	3.5–4.0
Potatoes, 60 cm high	4.0
Farmland, few trees	6.0
Farmland, many hedges	8.0
Bean crop, 1.2 m high	7.4
Cotton, 1.27 m high	13.0
Wheat	22.0
Citrus orchard	31.0–40.0
Corn, 2.2 m high	74.0
Blacktop, concrete	0.002
Airport runways	3.0
Highways, railways	50.0
Villages, towns	40.0–50.0
Residential, low density	110.0
City park	130.0
Urban, buildings, business district	175.0–320.0
High-rise apartments	370.0

From Hansen (1993b).

$$L'E = R_N - H - G. \quad (31)$$

With estimates of H and $L'E$, we are now in a position to compute C_n^2 as developed in the following section.

e. Flux–C_n^2 algorithm

The objective of this study is the application of radiation–energy balance modeling to estimate of the in-

tensity and character of optical turbulence as induced by atmospheric surface-layer processes. The following equations are presented in an effort to demonstrate our approach, wherein the temperature and moisture flux-gradient hypothesis is applied to computations of refractive-index gradients and in turn the refractive-index structure parameter. While the formulations in the literature are often obscured with unnecessary complexity, the following presentation should allow those familiar with the concepts of similarity scaling constants to readily digest its content.

The refractive index structure parameter can be expressed as in Tatarski (1961):

$$C_n^2(z) = b\frac{K_H}{\epsilon^{1/3}}\left(\frac{\partial n}{\partial z}\right)^2, \qquad (32)$$

where b is the Obukhov–Corrsin constant 3.2 (Panofsky 1968; Wyngaard 1973; Andreas 1988; Hill 1989); ϵ is the energy dissipation rate $u_*^3(\phi_m - \zeta)/kz$ (Panofsky 1968); z is the height above ground; K_H is the turbulent exchange coefficient for heat $u_*kz/\phi_H(\zeta)$; k is von Kármán's constant 0.4; u_* is the friction velocity; $\phi_H(\zeta)$ is the dimensionless lapse rate (Dyer 1974; Hicks 1976); $\phi_m(\zeta)$ is the dimensionless wind shear (Dyer 1974; Hicks 1976); ζ is scaling ratio z/L; L is the Obukhov scaling length $u_*^2\theta/kg\theta_{*v}$ (Busch 1973); θ is the potential temperature; θ_v^* is the virtual potential temperature scaling parameter; g is the gravitational acceleration; and $\partial n/\partial z$ is the gradient of the mean refractive index.

The expression we use for determining $\partial n/\partial z$ is based on expressions given by Andreas (1988). However, we

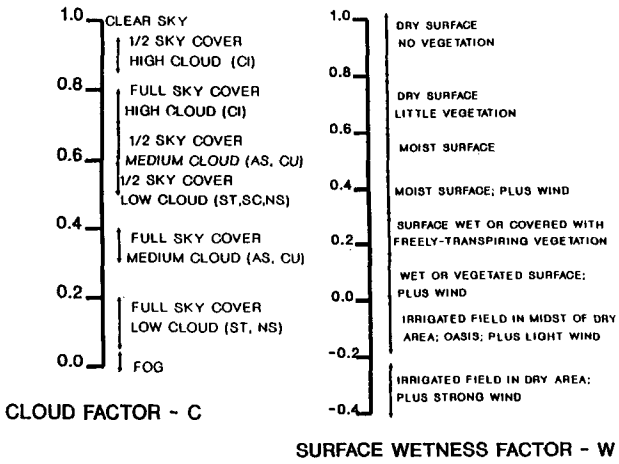

FIG. 1. Estimation of parameters C and W.

modified Andreas's formulations, which are expressed in terms of temperature and *absolute* humidity gradients, to expressions in terms of potential temperature and *specific* humidity gradients as required by Tatarski (1961). For the visible region and near-infrared wavelengths from 0.36 to 3 μm, Andreas (1988) writes

$$n_v = 1 + \left\{M_1(\lambda)\frac{P}{T} + 4.615[M_2(\lambda) - M_1(\lambda)]Q\right\} \times 10^{-6}, \qquad (33)$$

where

TABLE 7. Average thermal properties of soils, rock, snow, ice, and water.*

Material	State	K_s (W m^{-1} K^{-1})	K (m^2 h^{-1})	K_0 (W m^{-2} K^{-1})
Sand	Dry	0.277	9.000×10^{-4}	5.0
Sand	Moist	2.0	2.520×10^{-3}	20.8
Sand	Saturated	2.2	2.120×10^{-3}	24.3
Quartz sand (medium fine)	Dry	0.264	7.200×10^{-4}	5.037
Quartz sand	8.3% moist	0.586	1.188×10^{-3}	8.7
Yolo silt loam	Dry	0.12	4.500×10^{-4}	2.79**
Yolo silt loam	Moist	0.44	1.860×10^{-3}	5.23**
Yolo silt loam	Saturated	0.848	1.730×10^{-3}	10.44**
Sandy loam	Dry	0.23	5.760×10^{-4}	4.9
Sandy soil	Saturated	2.2	2.660×10^{-3}	21.8
Sandy clay	15% moist	0.925	1.330×10^{-3}	12.98
Clay soil	Dry	0.3	5.490×10^{-4}	6.28
Clay soil	Moist	1.47	3.960×10^{-3}	11.71
Clay soil	Saturated	1.58	1.840×10^{-3}	18.90
Clay pasture	—	2.76	4.320×10^{-3}	21.50
Calcareous soil (calcium carbonate)	43% water	0.712	6.480×10^{-4}	13.94
Soil (generic)	Very dry	0.167–0.345	$7.2–11.0 \times 10^{-4}$	3.19–5.37
Soil (generic)	Wet	1.260–3.350	$1.44–3.6 \times 10^{-4}$	17.0–28.6
Mud		0.84	7.920×10^{-4}	15.28
Peat soil	Dry	0.13	5.400×10^{-4}	2.65
Peat soil	Saturated	0.85	4.320×10^{-4}	20.95

* These values represent coarse averages of values taken from Oke (1978), Campbell (1977, 1985), Geiger (1965), Danard et al. (1984), Van Wijk (1963), and Lettau and Davidson (1957).

** These values are adjusted to approximate surface values.

$$M_1(\lambda) = 23.7134 + \frac{6839.397}{130 - \sigma^2} + \frac{45.473}{38.9 - \sigma^2} \quad (34)$$

$$M_2(\lambda) = 64.8731 + 0.58058\sigma^2 - 0.007115\sigma^4 + 0.0008851\sigma^6. \quad (35)$$

Here σ (μm) is λ^{-1}, Q (kg m^{-3}) is absolute humidity, P (mb) is pressure, and T (K) is temperature. Transforming Eq. (33) in terms of potential temperature θ and specific humidity q yields

$$n_v = 1 + \left\{ M_1(\lambda) \frac{P}{\theta - \gamma_d(z - z_r)} + 1.60948 \times [M_2(\lambda) - M_1(\lambda)] \frac{Pq}{\theta - \gamma_d(z - z_r)} \right\} \times 10^{-6}, \quad (36)$$

where z_r is the reference-level height, and γ_d is the dry-adiabatic lapse rate.

For steady-state, homogeneous conditions, Eq. (36) yields

$$\frac{\partial n}{\partial z} = \left\{ -M_1(\lambda) \frac{P}{T^2} - 1.61[M_2(\lambda) - M_1(\lambda)] \frac{Pq}{T^2} \right\} \times 10^{-6} \frac{\partial \theta}{\partial z} + 1.61[M_2(\lambda) - M_1(\lambda)] \frac{P}{T} \times 10^{-6} \frac{\partial q}{\partial z}, \quad (37)$$

where

$$\frac{\partial \theta}{\partial z} = \frac{\theta_*}{kz} \phi_H \quad \text{and} \quad \frac{\partial q}{\partial z} = \frac{q_*}{kz} \phi_H. \quad (38)$$

With this algorithm we use the modeled energy fluxes of sensible heat and latent heat to determine the similarity scaling constants for potential temperature and specific humidity as

$$\theta_* = -\frac{H}{\rho c_p u_*}; \quad q_* = -\frac{L'E}{\rho L' u_*}, \quad (39)$$

where ρ is air density, c_p is specific heat (c_p = 1004.6 J K^{-1} kg^{-1}), and L' is the latent heat of vaporization ($L' = 2.5 \times 10^6$ J kg^{-1}). We repeat our method for determining the surface friction velocity u_*, which we have shown to be equivalent to the methods presented by Paulson (1970) and Benoit (1977). Our method involves an iteration whereby after an initial guess for u_* (say, $u_* = 0.1V_r$, where V_r is the reference-level total horizontal wind speed), each successive estimate is approximated by

$$u_* = \frac{V_r k}{\{\ln[(x-1)/(x+1)] + 2\tan^{-1}(x)\}_{z_0}^{z_r}}, \quad (40)$$

where we redefine the Obukhov length as

$$L = \frac{-u_*^3 \theta_{vr} \rho c_p}{kg[H + 0.61\theta_r(L'E/L')]}. \quad (41)$$

In this expression for the Obukhov length, $\theta_{vr} = \theta_r(1 + 0.61q_r)$, where the r denotes the reference-level (i.e., 2 m) value. It is clear that given 2-m values for sensible heat, latent heat, wind speed, temperature, and specific humidity, one can numerically determine a value for the refractive-index structure parameter. Additionally, we have developed a simple method for determining the similarity scaling constants from multiple levels of discrete micrometeorological tower data (Rachele et al. 1992). The flux–C_n^2 algorithm can be modified to accommodate tower data gradients without significant difficulty.

4. Model results

The evaluation of our model is based on three sets of measured data (0.5-h averages) collected at Davis, California, during the summer of 1966 and spring of 1967 (Stenmark and Drury 1970; Brooks et al. 1968; Morgan et al. 1970). The Davis field site, a flat, 5-ha area at 17-m elevation above sea level, is located about 2 km west of the main portion of the University of California at the Davis campus, 24 km west of Sacramento, and 113 km northeast of San Francisco. The data were taken during periods when the surrounding fields were for the most part crop covered and well irrigated, giving, in effect, homogenous surface conditions with respect to temperature and moisture. Advection effects were considered to be negligible. Profiles of wind, temperature, and moisture were measured with transducers at nine levels from 25 to 600 cm. Raw data were processed to give 0.5-h average profiles.

In addition, 0.5-h values of net radiation and sensible, latent, and soil heat fluxes were available. The terrain at Davis was relatively smooth and covered with fescue grass (average height of 10 cm). The soil was assumed to be a silt loam and was moist. Two of the sets of data were collected during cloudless sky conditions.

Table 8 lists the constants from Tables 1, 2, 6, and 7 used for the model calculations. Two soil thermal constants are given to reflect the dry and damp soil flux calculations. For run 3, cloud-cover information was given in an appendix of Stenmark and Drury (1970).

Figure 2 shows the 0.5-h average values of reference-level temperature, relative humidity, and wind speed for the three days. Figures 3, 4, and 5 show the mea-

TABLE 8. Model constants as applied to Davis, California, data.

Albedo α	0.24
Emissivity ϵ	0.95
Roughness length z_0	1.4 cm
Thermal constant K_0	2.79; 3.55

sured and model values of sensible, latent, and ground heat fluxes for each day. Figure 6 shows the measured and modeled net radiation for each day. Figure 7 shows the results for the numerically approximated (at 2-m height) optical turbulence structure parameter (in the visible) for each day using measured versus modeled fluxes for inputs.

5. Discussion

It has already been mentioned that our model assumes that the sensible heat flux remains constant before sunrise and after sunset. Therefore, it is not surprising to see departures in our model estimates from the observed data at these times as shown in Figs. 3a and 3b. We do observe, however, a relatively uniform heat flux with time from midnight to sunrise, as suggested by Angus-Leppan (1971). With regard to Fig. 3c, it is clear that the structure of the observed data on this variably cloud-covered sky period has been reasonably well represented. Our success relies primarily upon our ability to interpret the cloud factor effects as shown in Fig. 1. One must consider the interrelation between the insolation ratios found in Table 4 and the cloud factors given in Fig. 1. Application of these corrections due to cloud cover depends heavily upon having good cloud opacity information as well as the more standard cloud base and cloud type input data. Imagine a partly cloudy sky over a given site of interest. One may experience the nearly complete blocking of the sun's rays. However, one may also observe a clear, unobstructed line of sight to the sun, even if $^8/_{10}$ or $^9/_{10}$ cloud cover were reported. We feel that this basic scenario has the potential for making radiation and energy balance modeling extremely difficult unless more effort is directed toward integrating cloud cover and ground wetness factors (Fig. 1) with the insolation ratio values of Haurwitz (1945) given in Table 4.

Remarkably good agreement between measured versus modeled values of latent heat flux are illustrated in Figs. 4a, 4b, and 4c, especially since $L'E$ is computed as the residual of the other estimated energy balance components. A strong dependency on Fig. 6c (net radiation) is implied by Fig. 4c.

The best results of ground heat flux estimates is shown in Fig. 5b. From each of the panels (5a, 5b, and 5c) it is clear that the expressions we have applied to this most difficult problem need refinement, especially at times of the day before sunrise and after sunset. The daytime peak magnitudes, however, are well represented, which we feel is primarily due to the proper application of the soil thermal constants given in Table 7.

Our most recognizable successes are illustrated in Figs. 6a, 6b, and 6c. We feel that the equations chosen for making estimates of the net radiative flux were well suited to our model constraints and ultimate application to electromagnetic propagation and imagery. As stated in the first paragraph of this section, we found

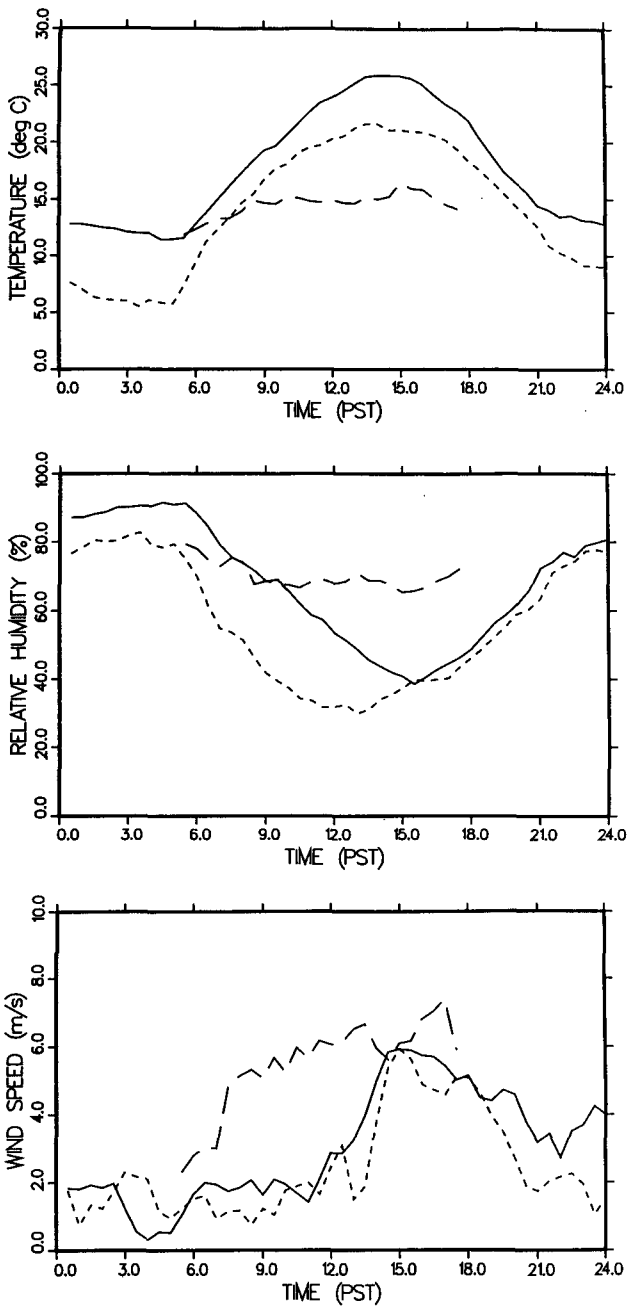

FIG. 2. The 0.5-h average values of reference-level (2 m) (a) temperature, (b) relative humidity, and (c) wind speed. Davis, California, data for 2 June 1966 (small dashed line), 13 July 1966 (solid line), and 9 May 1967 (large dashed line).

a sensitivity to modeling the net radiation under cloud-covered skies that relies heavily upon having good cloud opacity approximations. By using the information given in Table 4, we were able to adjust the calculated shortwave component to end up with better net radiation estimates. Once again, it is a more difficult task to model radiation exchanges when the cloud field is not uniform. The obscured or freely transmitted sun's

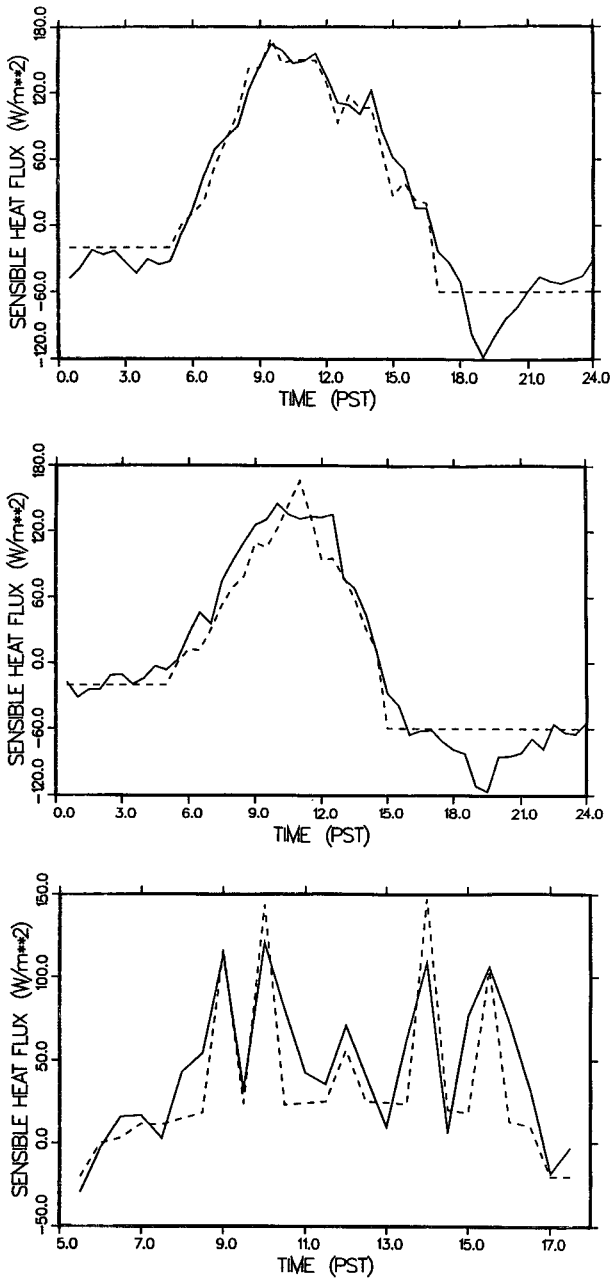

FIG. 3. Measured (solid line) and modeled (dashed line) values of sensible heat for Davis, California, data on (a) 2 June 1966, (b) 13 July 1966, and (c) 9 May 1967.

rays, regardless of the percentage of cloudiness observed, is the critical issue to be studied.

Finally, the estimates of C_n^2 using the measured versus modeled values of the sensible heat and latent heat fluxes seem to be in very good agreement, considering the complexity of the problem and the sensitivity of C_n^2 to the gradients of potential temperature and specific humidity. We feel that the structure, overall, during stable, unstable, and transition or neutral periods is very well represented.

6. Summary and conclusions

The purpose of this study was to determine the feasibility of structuring a radiation–energy balance model that would yield estimates of sensible and latent heat fluxes suitable for imagery and EM propagation assessments, research, and applications when constrained to require atmospheric measurement of temperature, pressure, relative humidity, and wind at a reference height (about 2 m) only. The model presented satisfies

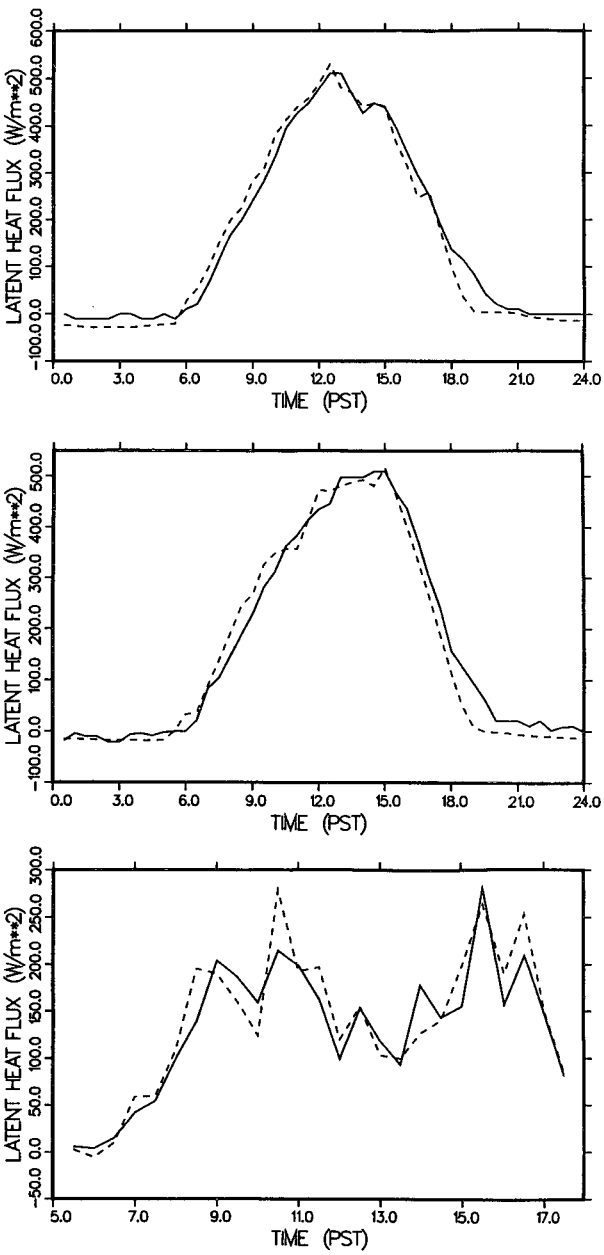

FIG. 4. Measured (solid line) and modeled (dashed line) values of latent heat for Davis, California, data on (a) 2 June 1966, (b) 13 July 1966, and (c) 9 May 1967.

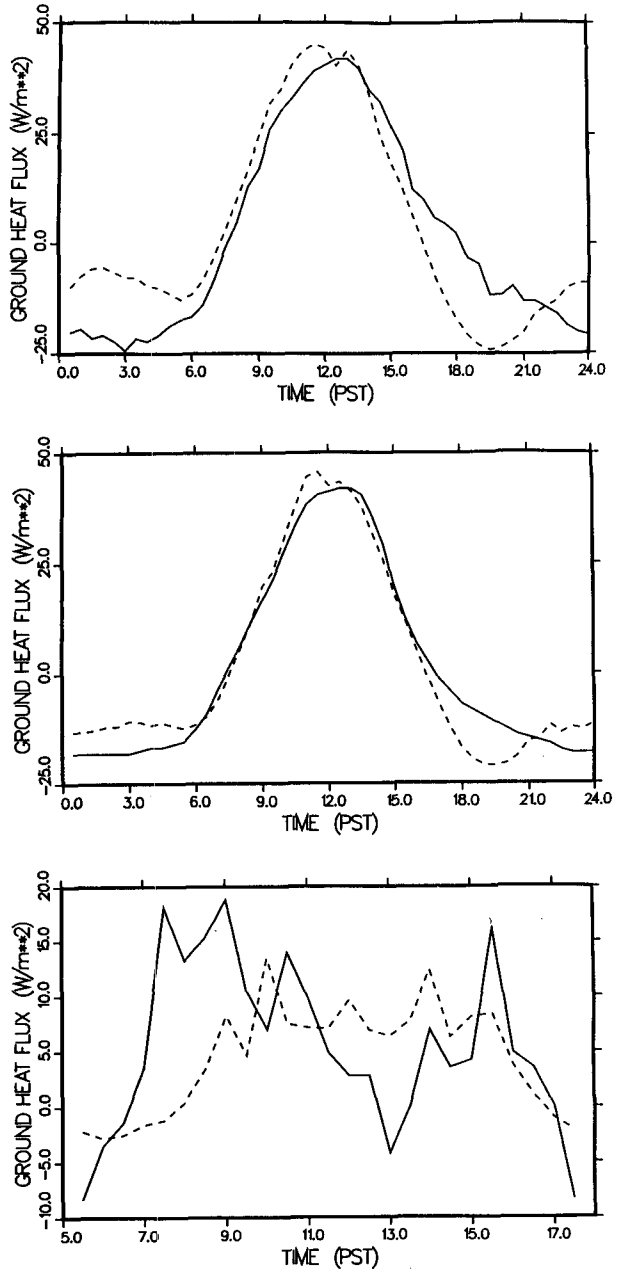

FIG. 5. Measured (solid line) and modeled (dashed line) values of ground heat flux for Davis, California, data on (a) 2 June 1966, (b) 13 July 1966, and (c) 9 May 1967.

the above constraints; however, one must also know the day of the year, time of day, longitude and latitude of the site of interest, soil type and moisture (dry, moist, saturated), and cloud characteristics (tenths of cloud cover, opacity, cloud type, and approximate height). The model is a composite of formulations, some purely physical and well founded, others semiempirical, and a few that are strictly empirical. Our major contributions include devising formulations for estimating ground heat flux and, most critically, tying together all the formulations and establishing a calculation procedure. The model is written in Fortran code and is fully annotated and available upon request from the authors. The run time for a 24-h calculation is less than 20 s on our laboratory HP-827 computer.

The three cases presented in this article were restricted to using data from Davis, California. Results are most encouraging for determining quantitative estimates of the radiation and energy balance fluxes as well as C_n^2 throughout the day over fescue grass. The

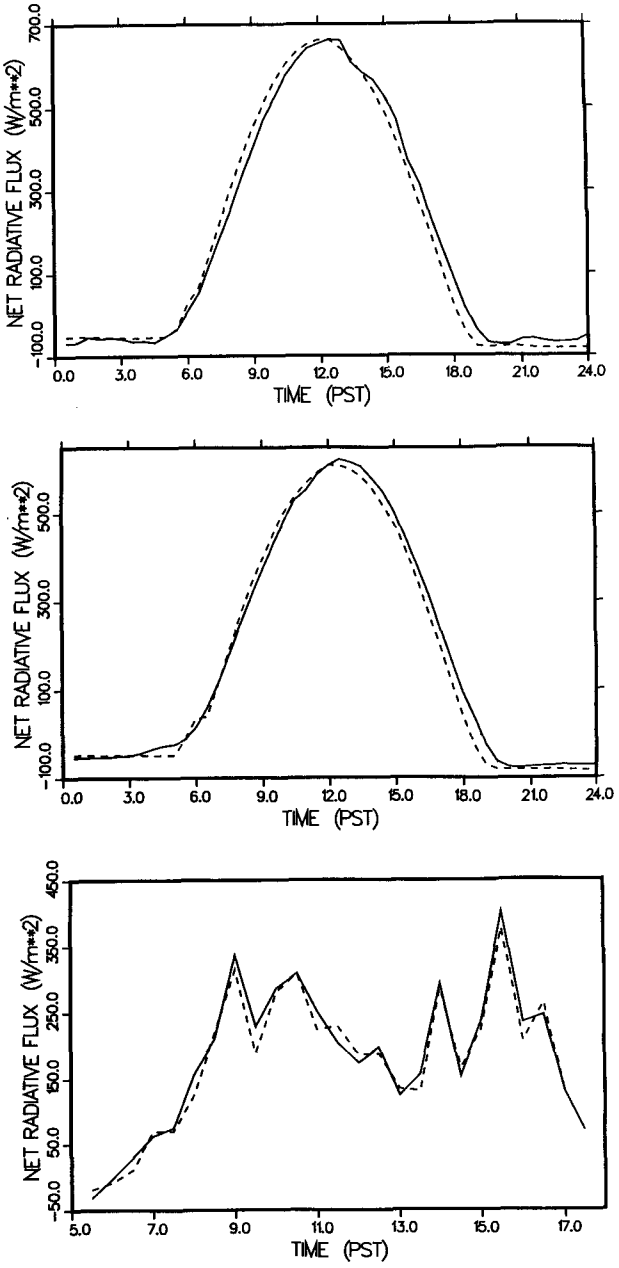

FIG. 6. Measured (solid line) and modeled (dashed line) values of net radiative flux for Davis, California, data on (a) 2 June 1966, (b) 13 July 1966, and (c) 9 May 1967.

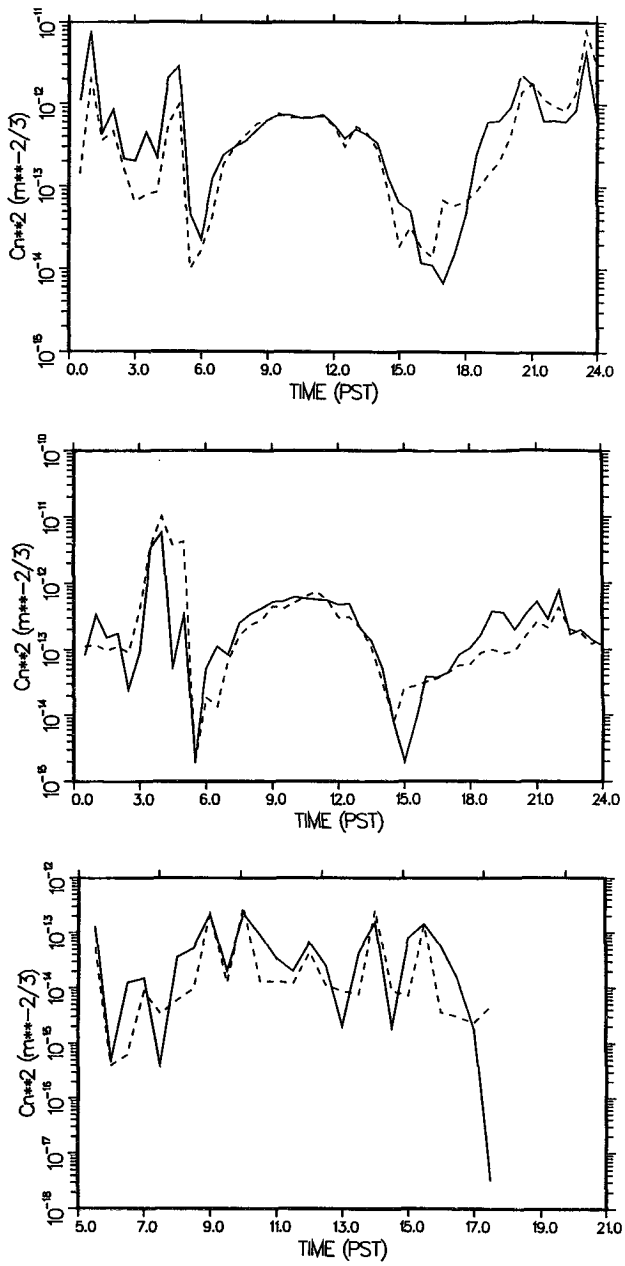

FIG. 7. The optical turbulence structure parameter C_n^2 for visible wavelengths (calculated at 2-m height) for Davis, California, data on (a) 2 June 1966, (b) 13 July 1966, and (c) 9 May 1967. Measured fluxes as input (solid line) and modeled fluxes as input (dashed line).

model is currently being refined for barren surfaces and other vegetative cover using data collected during a cooperative effort with the U.S. Department of Agriculture, Agricultural Research Service in May and July 1992 in Bushland, Texas (Tunick et al. 1994).

Acknowledgments. We thank Frank V. Hansen, formerly of ARL, for his willing and enthusiastic support and encouragement during the development of the model. He not only searched out many pertinent documents but also gave his time for discussion. We especially appreciate his efforts in compiling albedo and roughness length data for our tables.

REFERENCES

Andreas, E. L., 1988: Estimating C_n^2 over snow and sea ice from meteorological data. *J. Opt. Soc. Amer.*, **5,** 481–495.

Angus-Leppan, P. V., 1971: Meteorological physics applied to the calculation of refraction corrections. *Proc. Conf. of Commonwealth Survey Officers,* Cambridge, England, 107–111.

——, and F. K. Brunner, 1980: Atmospheric temperature models for short-range EDM. *The Canadian Surveyor,* **34,** 153–165.

Atwater, M. A., and P. Brown, 1974: Numerical calculation of the latitudinal variation of solar radiation for an atmosphere of varying opacity. *J. Appl. Meteor.*, **13,** 289–297.

Benoit, R., 1977: On the integral of the surface layer profile-gradient functions. *J. Appl. Meteor.*, **16,** 859–860.

Brooks, F. A., W. B. Goddard, and A. T. McDonald, 1968: Analysis in transfers of energy, momentum and moisture near the ground. U.S. Army Tech. Rep., ECOM-66-G26-F, 259 pp. [Available from U.S. Army Electronics Command, Atmospheric Sciences Laboratory, Fort Huachuca, AZ 85613.]

Busch, N. E., 1973: On the mechanics of atmospheric turbulence. *Workshop on Micrometeorology,* D. A. Haugen, Ed., Amer. Meteor. Soc., 1–65.

Campbell, G. S., 1977: *An Introduction to Environmental Biophysics.* Springer-Verlag, 159 pp.

——, 1985: *Soil Physics with Basic: Transport Models for Soil-Plant Systems.* Elsevier, 150 pp.

Carson, D. J., 1987: An introduction to the parameterization of land-surface processes: Part 1. Radiation and turbulence. *Meteor. Mag.*, **116,** 229–242.

Danard, M., G. Lyv, and G. MacGillivray, 1984: A mesoscale bulk model of the atmospheric boundary layer. Atmospheric Dynamics Corporation Report, 156 pp. [Available from Atmospheric Dynamics Corporation, 3052 Woodridge Place, R.R. 7, Victoria, British Columbia, Canada, V8X 3X3.]

Dyer, A. J., 1974: A review of flux-profile relationships. *Bound.-Layer Meteor.*, **1,** 363–372.

Fried, D. L., 1967: Propagation of a spherical wave in a turbulent medium. *J. Opt. Soc. Amer.*, **57,** 175–180.

Gates, D. M., 1965: Radiant energy, its receipt and disposal. *Agricultural Meteorology, Meteor. Monogr.*, No. 28, Amer. Meteor. Soc., 1–26.

Geiger, R., 1965: *The Climate Near the Ground.* Harvard University Press, 611 pp.

Hansen, F. V., 1993a: Albedos. ARL Tech. Rep. ARL-TR-57. [Available from U.S. Army Research Laboratory, Battlefield Environment Directorate, White Sands Missile Range, NM 88002-5501.]

——, 1993b: Surface roughness lengths. ARL Tech. Rep. ARL-TR-61. [Available from U.S. Army Research Laboratory, Battlefield Environment Directorate, White Sands Missile Range, NM 88002-5501.]

Haurwitz, B., 1945: Insolation in relation to cloudiness and cloud density. *J. Meteor.*, **2,** 154–166.

Hicks, B. B., 1976: Wind profile relationships from the Wangara experiment. *Quart. J. Roy. Meteor. Soc.*, **102,** 535–551.

Hill, R. J., 1989: Implications of Monin–Obukhov similarity theory for scalar quantities. *J. Atmos. Sci.*, **46,** 2236–2244.

Houghton, H. G., 1954: On the annual heat balance of the Northern Hemisphere. *J. Meteor.*, **11,** 1–9.

Kondratyev, K. Ya, 1969: *Radiation in the Atmosphere.* Academic Press, 912 pp.

Lettau, H. H., and B. Davidson, Eds., 1957: *Exploring the Atmosphere's First Mile.* Vol. 2. Pergamon Press, 578 pp.

McDonald, J. E., 1960: Direct absorption of solar radiation by atmospheric water vapor. *J. Meteor.*, **17,** 319–328.

Meyers, T. P., and R. F. Dale, 1983: Predicting daily insolation with hourly cloud height and coverage. *J. Climate and Appl. Meteor.*, **22,** 537–545.

Monin, A. S., and A. M. Obukhov, 1954: Basic regularity in turbulent mixing in the surface layer of the atmosphere. *Akad. Nauk. SSSR Trud. Geofiz. Inst.,* **24,** 151–179.

Morgan, D. L., W. O. Pruitt, and F. J. Lourence, 1970: Evaporation from an irrigated turf under advection of dry air at Davis, California. U.S. Army Tech. Rep., ECOM-68-G10-1. [Available from U.S. Army Electronics Command, Atmospheric Sciences Laboratory, Fort Huachuca, AZ 85613.]

Oke, T. R., 1978: *Boundary Layer Climates.* Methuen.

Paltridge, G. W., and C. M. R. Platt, 1976: *Radiative Processes in Meteorology and Climatology.* Elsevier Scientific, 318 pp.

Panofsky, H. A., 1968: The structure constant for the index refraction in relation to the gradient of index of refraction in the surface layer. *J. Geophys. Res.,* **73,** 6047–6049.

Paulson, C. A., 1970: The mathematical representation of wind speed and temperature profiles in the unstable atmospheric surface layer. *J. Appl. Meteor.,* **9,** 857–861.

Penman, H. L., 1948: Natural evaporation from open water bare soil and grass. *Proc. Roy. Soc. London,* **193,** 120–145.

Pielke, R. A., 1984: *Mesoscale Meteorological Modeling.* Academic Press, 612 pp.

Rachele, H., A. Tunick, and F. V. Hansen, 1992: The zephyrus, vaporous, thermotics connection. *Proc. 1992 Battlefield Atmospherics Conf.,* Ft. Bliss, TX, U.S. Army Research Laboratory, 59–78.

Rogers, R. R., 1979: *A Short Course in Cloud Physics.* 2d ed. Pergamon Press.

Smith, W. L., 1966: Note on the relationship between total precipitable water and surface dew point. *J. Appl. Meteor.,* **5,** 726–727.

Stenmark, E. B., and L. D. Drury, 1970: Micrometeorological field data from Davis, California 1966–67, runs under non-advective conditions. U.S. Army Tech. Rep., ECOM-6051, 604 pp. [Available from U.S. Army Electronics Command, Atmospheric Sciences Laboratory, Fort Huachuca, AZ 85613.]

Swinbank, W. C., 1963: Longwave radiation from clear skies. *Quart. J. Roy. Meteor. Soc.,* **89,** 339–348.

Tatarski, V. I., 1961: *Wave Propagation in a Turbulent Medium.* McGraw-Hill, 285 pp.

Tunick, A., H. Rachele, F. V. Hansen, T. A. Howell, J. L. Steiner, A. D. Schneider, and S. R. Evett, 1994: REBAL '92—A cooperative radiation and energy balance field study for imagery and electromagnetic propagation. *Bull. Amer. Meteor. Soc.,* **75,** 421–430.

Verma, S. B., 1989: Aerodynamic resistances to transfers of heat, mass, and momentum. *Proc. Workshop on Estimation of Areal Evapotranspiration,* Vancouver, IAHS, 13–20.

Webb, E. K., 1984: Temperature and humidity structure in the lower atmosphere. *Geodetic Refraction—Effects of Electromagnetic Wave Propagation through the Atmosphere,* F. K. Brunner, Ed., Springer-Verlag, 85–141.

Wesely, M. L., 1976: The combined effect of temperature and humidity fluctuations on refractive index. *J. Appl. Meteor.,* **15,** 43–49.

Van Wijk, W. R., 1963: General temperature variations in a homogeneous soil. *Physics of Plant Environment,* North-Holland, 144–170.

Woolf, H. M., 1968: On the computation of solar elevation angles on the determination of sunrise and sunset times. National Meteorological Center, Environmental Sciences Services Administration, Hillcrest Heights, MD.

Wyngaard, J. C., 1973: On surface layer turbulence. *Workshop on Micrometeorology,* D. A. Haugen, Ed., Amer. Meteor. Soc., 101–149.

Yamada, T., 1981: A numerical study of turbulent air flow in and above forest canopy. *J. Meteor. Soc. Japan,* **60,** 439–454.